Robust quantum random access memory

PHYSICAL REVIEW A **86**, 010306(R) (2012)

Robust quantum random access memory

Fang-Yu Hong,[1] Yang Xiang,[2] Zhi-Yan Zhu,[1] Li-zhen Jiang,[3] and Liang-neng Wu[4]

[1]*Department of Physics, Center for Optoelectronics Materials and Devices, Zhejiang Sci-Tech University, Hangzhou, Zhejiang 310018, China*

[2]*School of Physics and Electronics, Henan University, Kaifeng, Henan 475004, China*

[3]*College of Information and Electronic Engineering, Zhejiang Gongshang University, Hangzhou, Zhejiang 310018, China*

[4]*College of Science, China Jiliang University, Hangzhou, Zhejiang 310018, China*

(Received 11 January 2012; published 25 July 2012)

A "bucket brigade" architecture for a quantum random memory of $N = 2^n$ memory cells needs $n(n+5)/2$ times of quantum manipulation on control circuit nodes per memory call. Here we propose a scheme in which only on average $n/2$ times manipulations are required to accomplish a memory call. This scheme may significantly decrease the time spent on a memory call and the average overall error rate per memory call. A physical implementation scheme is discussed for storing an arbitrary state in a selected memory cell followed by reading it out.

DOI: 10.1103/PhysRevA.86.010306 PACS number(s): 03.67.Lx, 03.65.Ud, 03.67.Ac, 89.20.Ff

I. INTRODUCTION

A random access memory (RAM) is a fundamental computing device in which information (bits) can be stored in any memory cell and be read out at discretion [1,2]. A RAM is made up of an input address register, a data register, an array of memory cells, and a controlling circuit. A unique address is ascribed to each memory cell. When the address of a memory cell is loaded into the address register, the memory cell is selected and the information in the data register can be stored in it or the information about the cell can be read out to the data register. Like its classic counterpart, quantum random access memory (QRAM) is the building block of large quantum computers. A QRAM is a RAM working in a way with quantum characteristics: the address and data registers are comprised of qubits instead of bits, and every node of the controlling circuit is composed of a quantum object. When the address state is in superposition, $\sum_i \alpha_i |x_i\rangle$, the readout operation gives the output state $\sum_i \alpha_i |q_i\rangle$ in the data register, where $|q_i\rangle$ is the quantum information stored in the memory cell i associated with the address $|x_i\rangle$. QRAMs storing classic data can exponentially speed up pattern recognition [3–6], discrete logarithms [7,8], quantum Fourier transforms, and quantum searching on a classical database [9]. A general QRAM is indispensable for the performance of many algorithms, such as quantum searching [10], element distinctness [7,8], collision finding [11], general NAND-tree evaluation [12], and signal routing [13].

In seminal papers [13,14], Giovannetti, Lloyd, and Maccone (GLM) proposed a promising bucket-brigade architecture for QRAMs, which exponentially reduces the requirements for a memory call. However, in the GLM scheme, n times of quantum unitary transformations per memory call are required to turn one quantum trit initialized in $|\text{wait}\rangle$ in each node of the control circuit into $|\text{left}\rangle$ or $|\text{right}\rangle$, and all flying qubits including address qubits and bus qubits can pass through an arbitrary node of the controlling circuit only if a successful quantum manipulation has been performed on the trits, leading to the times of manipulations on the nodes $N_c = n(n+5)/2$ per memory call for 2^n memory cells, where n is the number of bits in the address register. Here we present a QRAM scheme, where the quantum object in every node has only two possible states $|\text{left}\rangle$ and $|\text{right}\rangle$. On average the times of quantum manipulations on the nodes per memory call can be reduced to $N_c = n/2$, significantly decreasing both the decoherence rate and the time spent on a QRAM call. A physical implementation for information storage and readout on a QRAM is presented.

II. QRAM PROTOCOL

The main idea is shown in Fig. 1. The N memory cells are positioned at the end of a bifurcation control circuit with $n = \log_2 N$ levels. At each node of the control circuit there is a qubit with two states $|\text{left}\rangle$ and $|\text{right}\rangle$. The state of the jth qubit in the address register controls which route to follow when a signal arrives at a node in the jth level of the circuit: if the address qubit is $|0\rangle$, the left path is chosen; if it is $|1\rangle$, the right path is chosen. For example, an address register $|001\rangle$ means left at the 1st level, left at the next, and right at the third. Illuminated by a control laser pulse, a node qubit in state $|\text{left}\rangle$ will flip to $|\text{right}\rangle$ if the incoming address qubit is $|1\rangle$, or remain in $|\text{left}\rangle$ if the address qubit is $|0\rangle$. Without the control pulse, a node qubit in $|\text{left}\rangle$ ($|\text{right}\rangle$) will deviate any incoming signal along the left (right) side route.

First, all the node qubits are initialized in state $|\text{left}\rangle$. Then the first qubit of the address register is dispatched through the circuit. At the first node, the address qubit incurs a unitary transformation U on the node qubit with the help of a control pulse $\Omega(t)$: $U|0\rangle|\text{left}\rangle = |0\rangle|\text{left}\rangle$ and $U|1\rangle|\text{left}\rangle = |0\rangle|\text{right}\rangle$. Next the second qubit of the address register is dispatched through the circuit, follows the left or right route relying on the state of the first node qubit, and arrives at one of the two nodes on the second level of the circuit. The node qubit illuminated by the control pulse will make a corresponding state change according to the state of the second address qubit, and so on. Note that the ith control pulse $\Omega(t)$ addresses all the nodes of the ith-level control circuit simultaneously. After all the n qubits of the address register have gone through the whole circuit, a unique path of n qubits has been singled out from the circuit (see Fig. 1). Subsequently, a single photon is sent along the selected path to single out a memory cell. After that an arbitrary unknown state in the data register can be transferred to the selected memory cell along the selected

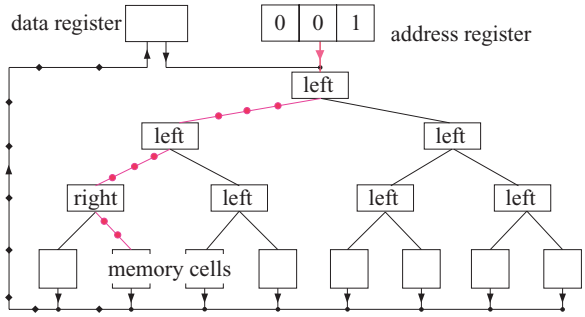

FIG. 1. (Color online) Schematics for a quantum random access memory. In each node of the binary control circuit, a qubit in $|\text{right}\rangle$ ($|\text{left}\rangle$) routes the approaching signals right (left). A single photon can excite the qubit from $|\text{left}\rangle$ to $|\text{right}\rangle$ with the aid of a classical impedance-matched control field $\Omega(t)$. Here the fourth-level memory cell $|001\rangle$ is addressed through the selected path marked with red circles. The readout state is transferred to a data register along the path marked with black squares.

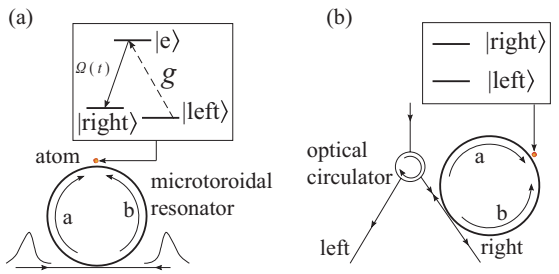

FIG. 2. (Color online) Schematic diagram of a node consisting of a three-level atom and a microtoroidal resonator. (a) An address qubit consisting of zero or one photon is split equally in counterpropagating directions and coherently stored using an impedance-matched control field $\Omega(t)$, leading to a state flip of the atom conditioned on the photon number. (b) By employing an optical circulator a photon traveling along a tapered fiber that is in critical coupling to the resonator will go along the left (right) path if the atom is in state $|\text{left}\rangle$ ($|\text{right}\rangle$).

path, or the state of the selected memory cell can be read out to the data register along the path with black squares in Fig. 1. Finally, all the node qubits are reset to $|\text{left}\rangle$ for a next memory address.

Because the state of a node qubit $|\text{left}\rangle$ will not be affected by the illuminating control pulse should the address qubit be in state $|0\rangle$, where there is no interaction between the address qubit and the node qubit, on average there are $n/2$ node qubits that will flip to $|\text{right}\rangle$ in each memory call. This means that on average only $n/2$ times of control manipulations are really performed in each memory call. As a result, the mean comprehensive error rate per memory address is $n\epsilon/2 = \frac{1}{2}\log_2 N\epsilon$ with the assumed error rate ϵ per node qubit flip event. In contrast, the GLM scheme requires n times state flips for a memory call. In addition, in the GLM scheme a photon may pass through a node only when a control pulse is applied on the quantum trit, causing the overall times of quantum manipulations on the quantum trits per memory call to be $n(n+5)2$, which includes $2n$ times of manipulations for a signal photon going to a memory cell and back to a data register along the same selected path. Here a single photon can pass through a node without any quantum manipulation; therefore the average times of quantum manipulation really performed on node qubits per memory call is $n/2$. Thus this scheme may significantly decrease the average overall error rate and shorten the time required for a memory call.

III. PHYSICAL IMPLEMENTATION

Now we discuss a possible physical implementation. The node qubit is encoded on an atom with levels $|\text{left}\rangle$, $|\text{right}\rangle$, and an intermediate state $|e\rangle$ [see Fig. 2(a)]. The transition between $|\text{left}\rangle$ and $|e\rangle$ is coupled to the evanescent fields of modes a and b of frequency ω_c of a microtoroidal resonator, into and out of which photons can be coupled with high efficiency of 99.9% [15]. The state $|\text{right}\rangle$ is coupled to $|e\rangle$ by the classical control field $\Omega(t)$. A tapered fiber and the resonator are assumed to be in critical coupling where the input photons of frequency $\omega_p = \omega_c$ are all reflected back and the forward flux in the fiber drops to zero when the atom transition ($|\text{left}\rangle \rightarrow |e\rangle$) is far detuned from the resonator frequency ω_c [16]. If the atomic transition ($|\text{right}\rangle \rightarrow |e\rangle$) is on resonance with the resonator, the input photons can transmit the resonator and travel forward one by one [17]. A single photon can be coherently stored in the atom initialized in $|\text{left}\rangle$ by applying the control pulse $\Omega(t)$ simultaneously with the arrival of the photon which is equally divided and incident from both sides of the tapered fiber simultaneously (see Fig. 2) [18]. The photon storage can be completed within 0.5 μs and results in a state flip of the atom to $|\text{right}\rangle$, or the atom remains in $|\text{left}\rangle$ for the case with no single photon contained in the incoming field [18].

The switch function of a node qubit in a QRAM can be realized as follows: First, the address qubit is encoded as $\alpha|0\rangle_p + \beta|1\rangle_p$ with Fock state $|n\rangle_p$ ($n = 0,1$) and arbitrary unknown complex coefficients α and β; the first qubit of the address register is sent out along the control circuit and is coherently stored in the atom in the first node by applying the control pulse $\Omega(t)$ simultaneously with the arrival of the address qubit equally split and incident from both sides of the tapered fiber simultaneously. This storing process will incur a state flip of the node atom to $|\text{right}\rangle$ if the address qubit is $|1\rangle$, or make no change in the atom state $|\text{left}\rangle$ if the address qubit is $|0\rangle$. When the second address qubit is sent out and meets the first node, it will be reflected back and travel along the left path by application of an optical circulator in one side of the tapered fiber [Fig. 2(b)] if the atom in the first node is in $|\text{left}\rangle$, or will transmit through the resonator and go along the right path if the atom is in $|\text{right}\rangle$. When the second address qubit arrives at one of the two nodes on the second level, it will be coherently stored in the node atom and leave the atom in $|\text{left}\rangle$ or $|\text{right}\rangle$ depending on the photon number contained in the address qubit, and so on.

We assume that each quantum memory cell in the memory array consists of a memory atom m and an ancillary atom a, which are confined in two harmonic traps and positioned inside a high-quality cavity [Fig. 3(a)]. The atom confinement can be supplied either by far-off-resonance optical traps (FORTs) defined by tightly focusing laser light in a set of chosen locations [19,20] or by permanent magnetic microtraps designed on patterned permanently magnetized thin films [21,22]. In addition to a metastable level $|t\rangle_a$ and two Rydberg

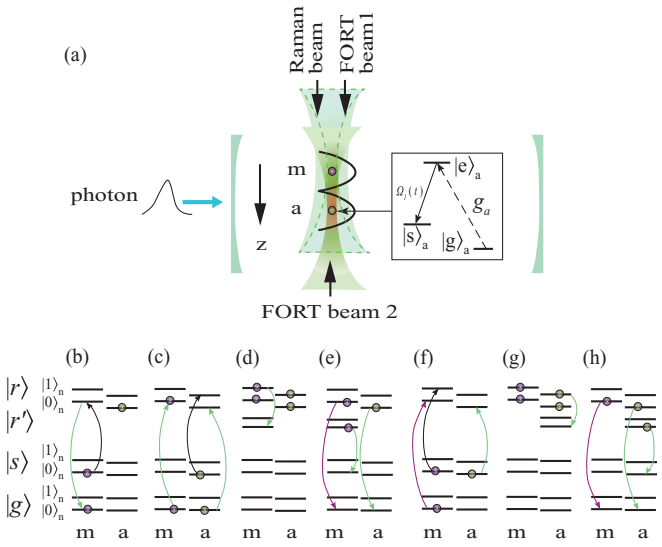

FIG. 3. (Color online) Schematics for memory writing and readout. (a) With the help of a time-dependent control pulse propagating along the $\hat{z}$ direction, a single photon can be coherently stored in atom a in a memory cell consisting of atoms m and a. Positioned inside a high-Q cavity, atoms m and a are confined in two harmonic traps provided by FORT pulses 1 and 2, respectively, which propagate along the $\hat{z}$ direction. (b)–(e) Diagrams of energy levels and pulse sequences for transfer of an unknown state of atom a to atom b in the selected memory cell. (f)–(h) The concerned energy levels and pulse sequences for transfer of an unknown state of atom m to atom a in the selected memory cell.

levels $|r\rangle_a$ and $|r'\rangle_a$, the ancillary atom has a three-level structure: $|g\rangle_a$ is coupled to $|e\rangle_a$ by the field of the cavity mode with strength g_a; $|s\rangle_a$ is coupled to $|e\rangle_a$ by a classic control field $\Omega_1(t)$, where the subscript a denotes an ancillary atom. After a path to the memory array is singled out, a single photon is sent along the path to the selected memory cell. A control laser pulse $\Omega_1(t)$ is applied to the ancillary atoms initialized in state $|g\rangle_a$ at the moment when the photon arrives at the memory cell, resulting a state flip of atom a to $|s\rangle_a$ [23,24]. This whole photon absorption process can be completed within 300 ps [23]. To avoid being involved in the quantum operations aimed at the selected memory cell, the ancillary atoms nonselected are excited to a stable state $|t\rangle_a$ by a π pulse on the transition $|g\rangle_a \rightarrow |t\rangle_a$. Next we can do some quantum manipulations either to save an arbitrary unknown quantum state in the selected memory cell or to read out its content.

In the first place, we discuss how to save an arbitrary unknown quantum state in the memory cell identified by the address register. First, an initialization operation on the memory cell array is performed. This can be realized as follows: Atom a in state $|s\rangle_a$ is excited to a Rydberg state $|r\rangle_a$ by a π two-photon stimulated Raman (TPSR) pulse [$\int \Omega_f(\tau)d\tau = \pi$] with effective Rabi frequency $\Omega_f(\tau)$ propagating along the $\hat{z}$ direction [Fig. 3(a)] [19,20,25]. A π TPSR pulse on the transition $|s\rangle_m \rightarrow |r\rangle_m$ (in terms of the perturbed state) of the memory atoms is applied, resulting in the selected memory atom m being excited to $|r\rangle_m$ and immediately flipping to the ground state $|g\rangle_m$ by the illumination of another π TPSR pulse on the transition $|r\rangle_m \rightarrow |g\rangle_m$ [Fig. 3(b)] [26,27]. In this way only the memory atom in the selected memory cell is reset in state $|g\rangle_m$, leaving the content of the others unchanged, because the states $|r\rangle_m$ of the nonselected memory atoms are off resonance with the TPSR pulse due to the absence of the strong Rydberg dipole interactions [28]. The ancillary atom in Rydberg state $|r\rangle_a$ is brought to the ground state $|g\rangle_a$ by applying a π TPSR pulse on its transition $|r\rangle_a \rightarrow |g\rangle_a$.

Second, an arbitrary unknown state $\alpha|0\rangle_p + \beta|1\rangle_p$ with Fock bases $|n\rangle_p$ $(n = 0,1)$ is transferred along the selected path to the memory cells. On the arrival of the signal a classic control pulse $\Omega_2(t)$ is applied on the ancillary atoms initialized in the ground state $|g\rangle_a$, leading to a state map $(\alpha|0\rangle_p + \beta|1\rangle_p)|g\rangle_a \rightarrow |0\rangle_p(\alpha|g\rangle_a + \beta|s\rangle_a)$ [23,24].

The state $\alpha|g\rangle_a + \beta|s\rangle_a$ is then transferred to the chosen memory atom m by employing the strong dipole interaction between two Rydberg atoms [29,30]. When both of the memory atom and the ancillary atom contained in two harmonic traps are in Rydberg states, the strong dipole interaction between them will couple their external motions along the $\hat{z}$ direction [Fig. 3(a)]. This coupled motion of the two atoms is best described in the basis of normal modes $|j\rangle_n$ $(j = 0,1,2,\ldots)$. All the motion modes of the atoms are initially cooled to near their ground state by Raman sideband cooling [31].

Third, we drive a π pulse on the transition $|g\rangle_m \rightarrow |r\rangle_m$ on the memory atoms to excite them from state $|g\rangle_m$ to state $|r\rangle_m$. Fourth, a π pulse on the transition $|g\rangle_a \rightarrow |r\rangle_a|0\rangle_n$ and a blue sideband pulse on the transition $|s\rangle_a \rightarrow |r\rangle_a|1\rangle_n$ are applied on the ancillary atoms, leading to the state

$$|\psi\rangle_1 = \alpha|r\rangle_a|r\rangle_m|0\rangle_n + \beta|r\rangle_a|r\rangle_m|1\rangle_n \qquad (1)$$

for the selected memory cell and the state $|\psi\rangle_2 = (\alpha_x|r\rangle_m + \beta_x|s\rangle_m)|t\rangle_a$ for other memory cells with their initial states $\alpha_x|g\rangle_m + \beta_x|s\rangle_m$ [Fig. 3(c)]. Here we have used the fact that the normal mode of motion is shared by atoms m and a in the selected memory cell, both of which are in Rydberg states. Fifth, a π pulse on the transition $|r\rangle_m \rightarrow |g\rangle_m$ unperturbed by the strong dipole interaction between two Rydberg atoms is applied on the nonselected memory atoms to restore them to their initial states $\alpha_x|r\rangle_m + \beta_x|s\rangle_m$.

Sixth, a π pulse on the transition $|r\rangle_m|1\rangle_n \rightarrow |r'\rangle_m|0\rangle_n$ illuminates the memory atoms [Fig. 3(d)], resulting in a state mapping

$$|\psi\rangle_1 \rightarrow |\psi\rangle_3 = \alpha|r\rangle_a|r\rangle_m|0\rangle_n + \beta|r\rangle_a|r'\rangle_m|0\rangle_n. \qquad (2)$$

Seventh, two π pulses on $|r'\rangle_m \rightarrow |s\rangle$ and $|r\rangle_m \rightarrow |g\rangle_m$, respectively, are applied on the memory atom, leading to a unitary transformation $|\psi\rangle_3 \rightarrow |\psi\rangle_4 = (\alpha|g\rangle_m + \beta|s\rangle_m)|r\rangle_a$ [Fig. 3(e)]; the unknown state $\alpha|0\rangle + \beta|1\rangle$ has been stored on the selected memory atom. Note that these two pulses in the seventh stage will not affect the states of the nonselected memory atoms since the pulses are detuned from their transitions $|r'\rangle_m \rightarrow |s\rangle_m$ and $|r\rangle_m \rightarrow |g\rangle_m$, which are free of the influence of strong dipole interaction between two Rydberg atoms. Eighth, the ancillary atom is restored to the ground state $|g\rangle_a$ by a π pulse on the transition $|r\rangle_a \rightarrow |g\rangle_a$ [Fig. 3(e)], and the nonselected ancillary atoms are restored to the ground state $|g\rangle$ for the next memory call by a π pulse on the transition $|t\rangle_a \rightarrow |g\rangle_a$. In this way an arbitrary unknown state can be

transferred to the selected memory atom, leaving the states of other memory atoms unchanged.

Now we discuss how to read out the content of the selected memory atom $\alpha_x|g\rangle_m + \beta_x|s\rangle_m$. First, a π pulse on the transition $|s\rangle_a \rightarrow |r\rangle_a$ is employed to excite the selected ancillary atom to state $|r\rangle_a$. Second, we employ two π pulses on the transitions $|g\rangle_m \rightarrow |r\rangle_m|0\rangle_n$ and $|s\rangle_m \rightarrow |r\rangle_m|1\rangle_n$, respectively [Fig. 3(f)], driving the system of the selected atoms m and a into the state

$$|\psi\rangle_5 = \alpha_x|r\rangle_m|r\rangle_a|0\rangle_n + \beta_x|r\rangle_m|r\rangle_a|1\rangle_n. \quad (3)$$

Third, a π pulse on the transition $|r\rangle_a|1\rangle_n \rightarrow |r'\rangle_a|0\rangle_n$ drives the selected system into the state $|r\rangle_m(\alpha_x|r\rangle_a + \beta_x|r'\rangle_a)|0\rangle_n$ [Fig. 3(g)]. Fourth, the selected memory atom is sent to the ground state by a π pulse on the transition $|r\rangle_m \rightarrow |g\rangle_m$. Fifth, two pulses on the transitions $|r\rangle_a \rightarrow |g\rangle_a$ and $|r'\rangle_a \rightarrow |s\rangle_a$, respectively, set the selected ancillary atom in the state $\alpha_x|g\rangle_a + \beta_x|s\rangle_a$ [Fig. 3(h)]; the content of the selected memory atom is transferred to atom a in the selected memory cell. Note that these pulses do not influence the nonselected atoms a and m because the former have no strong dipole interaction and the latter are in state $|t\rangle_a$. By applying a classical impedance-matched control field $\Omega(t)_3$, a matter-photon mapping $(\alpha_x|g\rangle_a + \beta_x|s\rangle_a)|0\rangle_p \rightarrow |g\rangle_a(\alpha_x|0\rangle_p + \beta_x|1\rangle_p)$ can be accomplished within 300 ps [23,24], transferring the state of the selected memory cell to the flying qubit and leaving the ancillary atom in state $|g\rangle_a$. The flying qubit goes along the path with black squares to the data register (Fig. 1). Finally, the nonselected ancillary atoms are initialized to state $|g\rangle_a$ for the next task.

The π TPSR pulses for the transitions between the normal mode states $|1\rangle \leftrightarrow |0\rangle$ can be completed within 6 μs [29], while other π TPSR pulses can be accomplished within 0.1 μs [25], so that the process of state transfer between atoms a and m can be finished in less than 13 μs. Considering the time spent on the route-selecting process we can carry out a memory address within 30 μs for a QRAM of 2^{32} memory cells.

IV. CONCLUSIONS

In summary, we have presented a scheme for a quantum random access memory. The three-level memory system has been substituted by a qubit in every node of the control circuit, and this structure may significantly reduce the overall error rate per memory address and the memory address time. In addition, we have discussed a physical implementation based on a microtoroidal resonator and strong dipole interaction between two trapped Rydberg atoms in a high-Q cavity for a QRAM writing and readout. The microtoroidal resonator and the tapered fiber may be replaced by a surface plasmon propagating on the surface of a nanowire-conductor-dielectric interface [32,33].

ACKNOWLEDGMENTS

This work was supported by the National Natural Science Foundation of China (Grants No. 11072218 and No. 11005031), by the Zhejiang Provincial Natural Science Foundation of China (Grants No. Y6110314 and No. Y6100421), and by the Scientific Research Fund of Zhejiang Provincial Education Department (Grants No. Y200909693 and No. Y200906669).

[1] R. Feynman, *Feynman Lectures on Computation* (Perseus Books, New York, 2000).
[2] R. C. Jaeger and T. N. Blalock, *Microelectronic Circuit Design* (McGraw-Hill, Dubuque, 2003), p. 545.
[3] G. Schaller and R. Schützhold, Phys. Rev. A **74**, 012303 (2006).
[4] R. Schützhold, Phys. Rev. A **67**, 062311 (2003).
[5] C. A. Trugenberger, Phys. Rev. Lett. **87**, 067901 (2001); **89**, 277903 (2002).
[6] D. Curtis and D. A. Meyer, Proc. SPIE **5161**, 134 (2004).
[7] A. Ambainis, in *Proceedings of the 45th IEEE Symposium on Foundations of Computer Science (FOCS'04)* (IEEE Computer Society, Rome, 2004), p. 22; SIAM J. Comput. **37**, 210 (2007).
[8] A. M. Childs, A. W. Harrow, and P. Wocjan, *Lecture Notes in Computer Science*, Vol. 4393 (Springer, New York, 2007), p. 598.
[9] M. A. Nielsen and I. L. Chuang, *Quantum Computation and Quantum Information* (Cambridge University Press, Cambridge, 2000).
[10] L. K. Grover, in *Proceedings of the 28th Annual Symposium on the Theory of Computing* (ACM Press, New York, 1996), p. 212.
[11] G. Brassard, P. Høer, and A. Tapp, ACM SIGACT News **28**, 14 (1997).
[12] A. M. Childs *et al.*, arXiv:quant-ph/0703015 [in *Proceedings of the 48th IEEE Symposium on Foundations of Computer Science (FOCS07)* (to be published)].
[13] V. Giovannetti, S. Lloyd, and L. Maccone, Phys. Rev. A **78**, 052310 (2008).
[14] V. Giovannetti, S. Lloyd, and L. Maccone, Phys. Rev. Lett. **100**, 160501 (2008).
[15] S. M. Spillane, T. J. Kippenberg, O. J. Painter, and K. J. Vahala, Phys. Rev. Lett. **91**, 043902 (2003).
[16] T. Aoki, B. Dayan, E. Wilcut, W. P. Bowen, A. S. Parkins, T. J. Kippenberg, K. J. Vahala, and H. J. Kimble, Nature (London) **443**, 671 (2006).
[17] B. Dayan, A. S. Parkins, T. Aoki, E. P. Ostby, K. J. Vahala, and H. J. Kimble, Science **319**, 4062 (2008).
[18] F.-Y. Hong and S.-J. Xiong, Phys. Rev. A **78**, 013812 (2008).
[19] E. Urban, T. A. Johnson, T. Henage, L. Isenhower, D. D. Yavuz, T. G. Walker, and M. Saffman, Nat. Phys. **5**, 110 (2009).
[20] M. Saffman and T. G. Walker, Phys. Rev. A **72**, 022347 (2005).
[21] R. Schmied, D. Leibfried, R. J. C. Spreeuw, and Shannon Whitlock, New J. Phys. **12**, 103029 (2010).
[22] A. Mohammadi and S. Ghanbari, arXiv:1101.6068v1.
[23] W. Yao, R.-B. Liu, and L. J. Sham, Phys. Rev. Lett. **95**, 030504 (2005).

[24] W. Yao, R.-B. Liu, and L. J. Sham, J. Opt. B: Quantum Semiclassical Opt. **7**, S318 (2005).

[25] A. Gaëan, Y. Miroshnychenko, T. Wilk, A. Chotia, M. Viteau, D. Comparat, P. Pillet, A. Browaeys, and P. Grangier, Nat. Phys. **5**, 115 (2009).

[26] M. D. Lukin, M. Fleischhauer, R. Cote, L. M. Duan, D. Jaksch, J. I. Cirac, and P. Zoller, Phys. Rev. Lett. **87**, 037901 (2001).

[27] E. Brion, K. Mølmer, and M. Saffman, Phys. Rev. Lett. **99**, 260501 (2007).

[28] D. Jaksch, J. I. Cirac, P. Zoller, S. L. Rolston, R. Côté, and M. D. Lukin, Phys. Rev. Lett. **85**, 2208 (2000).

[29] F.-Y. Hong, Y. Xiang, Z. Y. Zhu, and W. H. Tang, Quantum Inf. Comput. **11**, 0925 (2011).

[30] P. O. Schmidt, T. Rosenband, C. Langer, W. M. Itano, J. C. Bergquist, and D. J. Wineland, Science **309**, 749 (2005).

[31] C. Monroe, D. M. Meekhof, B. E. King, W. M. Itano, and D. J. Wineland, Phys. Rev. Lett. **75**, 4714 (1995).

[32] D. E. Chang, A. S. Sørensen, E. A. Demler, and M. D. Lukin, Nat. Phys. **3**, 807 (2007).

[33] F.-Y. Hong and S. J. Xiong, Nanoscale Res. Lett. **3**, 361 (2008).